

International Journal of Modelling, Identification and Control

ISSN online: 1746-6180 - ISSN print: 1746-6172
<https://www.inderscience.com/ijmic>

A novel adaptive variable speed control strategy for wound rotor induction motors

Dieudonné Ekan, Donatien Nganga-Kouya, Aime Francis Okou

DOI: [10.1504/IJMIC.2023.10053832](https://doi.org/10.1504/IJMIC.2023.10053832)

Article History:

Received:	18 August 2021
Last revised:	27 December 2021
Accepted:	30 January 2022
Published online:	03 February 2023

A novel adaptive variable speed control strategy for wound rotor induction motors

Dieudonné Ekang* and Donatien Nganga-Kouya

Department of Electrical Engineering,
Ecole Normale Supérieure de l'Enseignement Technique of Gabon,
Leon Mba Boulevard, Libreville, BP 3989, Gabon
and

Mechanical Engineering Department,
Ecole Normale Supérieure de l'Enseignement Technique of Gabon,
Leon Mba Boulevard, Libreville, BP 3989, Gabon
Email: dieudonnekang@gmail.com
Email: ngad1109@yahoo.com

*Corresponding author

Aime Francis Okou

Department of Electrical and Computer Engineering,
Royal Military College of Canada,
13 General Crerar Crescent, Kingston,
Ontario, K7K 7B4, Canada
Email: aime.okou@rmc.ca

Abstract: A new approach is proposed for the design of an adaptive variable speed controller for an induction motor. This design approach is based on a new model for induction motors in the (α/β) reference frame. The model state variables are constant in steady state and therefore enable the application of adaptive backstepping control design techniques to find controller equations and adaptation laws that ensure that the rotor speed and flux track their reference values despite significant changes in machine resistances and inductances due to temperature and magnetic saturation. The proposed controller is tested in simulation. Results show robust steady state and transient performances.

Keywords: wound rotor of induction motor; adaptive backstepping control; speed control; rotor flux control; stability analysis.

Reference to this paper should be made as follows: Ekang, D., Nganga-Kouya, D. and Okou, A.F. (2023) 'A novel adaptive variable speed control strategy for wound rotor induction motors', *Int. J. Modelling, Identification and Control*, Vol. 42, No. 1, pp.31–45.

Biographical notes: Dieudonné Ekang obtained his Master's degree and PhD in Electrical Engineering from the Ecole Normale Supérieure de l'Enseignement Technique (ENSET) in Libreville, Gabon in 2016 and 2021, respectively. He is a member of the LARTESY Laboratory. His research interests focus on linear and nonlinear control techniques applied to electric machines.

Donatien Nganga-Kouya received his Master's degree in Engineering in 1996 and PhD in Engineering in 2003 from the École de Technologie Supérieure (ÉTS) of the University of Quebec Canada. He is a Senior Lecturer at ENSET Libreville and an expert of the Specialised Technical Committee of CAMES Engineering Sciences and Techniques. He is the Director of the Systems Technology Research Laboratory (LARTESY) at ENSET. His research interests are in automation, systems control and technology.

Aime Francis Okou received his Diplôme d'Ingénieur degree in Electrical Engineering from École Supérieure Interafricaine de l'Électricité, Côte d'Ivoire in 1993, MEng degree and PhD in Electrical Engineering from École de Technologie Supérieure (ÉTS), Montreal, QC, Canada in 1996 and 2001, respectively. During 2002–2005, he was a Postdoctoral Researcher in the Department of Electrical Engineering at ÉTS. Since 2005, he joined The Royal Military College of Canada where he is currently a Full Professor in the Electrical and Computer Engineering Department. His research interests include the application of robust adaptive nonlinear control techniques to power systems and robotic systems.

1 Introduction

Many industrial electromechanical drive systems such as fans and conveyor belts use induction motors (Saravanan et al., 2012). These AC motors have gradually replaced DC motors because of their low purchase and maintenance costs, and their high reliability (Costa et al., 2018; Traoré et al., 2012). However, the design of high-performance variable speed control systems for induction machines is still an open challenge for researchers and engineers. The complexity of the problem is that induction machines are nonlinear time-varying parameter systems due to the magnetic core saturation and operating temperature that change the machine inductances and resistances with operation conditions. It is therefore very common to make simplifying assumptions to design a control system for an induction machine. The magnetic core is generally assumed linear which implies that machine inductances are fixed and the effects of temperature on machine resistances are sometimes neglected.

The literature reports several methods that have been proposed for the design of variable speed control of induction machines. One can distinguish the conventional scalar controls (Derouich and Lagrioui, 2014; Jannati et al., 2017; Dos Santos et al., 2014), vector controls (El Ouanjli et al., 2017; Nishad and Sharma, 2018), input-output linearisation controls (Chiasson, 1993; Chiasson, 1998; Marino et al., 2010), direct torque controls (DTC) (Takahashi and Noguchi, 1986; Depenbrock, 1987), sliding mode controls (Horch et al., 2019) and backstepping controls (Krstic et al., 1995; Okou et al., 2009; Khalil and Grizzle, 2002; Liu et al., 2020). Although these control methods provide good dynamic performances, they remain very sensitive to changes in machine parameters. They are based on simplified induction machine models in which rotor and stator resistances as well as rotor, stator inductances and the mutual inductance are assumed known and constant. However, in practice, these parameters can change during the machine operation (Ebrahim and Murphy, 2010). For stator and rotor resistances, the increase in temperature and the skin effect can cause a change up to 50% of the rated values (Chen and Huang, 2016). For inductances, the change in rotor flux due to the magnetic core saturation can cause a change up to $\pm 20\%$ of the rated values (Mengoni et al., 2012). The difference between controller parameters and actual machine parameters greatly reduces the performance of the controller and in some cases can even destabilise the closed loop system.

The literature reports several robust or adaptive control variable speed control drives to address the aforementioned issue. Indeed, in Fateh and Abdellatif (2017), Mehazzem et al. (2011), Hajji et al. (2019), Aichi et al. (2020) and Horch et al. (2017), the authors use integrators in the control loop to reduce the speed and flux errors in steady and thus improve the system robustness. However, the integrators increase the complexity of the proposed control system and the stator resistance and inductance are assumed constant during simulations. In Belkheiri and Boudjema (2008), the authors propose a control approach to address the tracking

problem of an induction machine based on a modified field-oriented control (FOC) method. A backstepping control strategy augmented by an adaptive neural network (NN) is used. Neural network weights are adjusted using adaptation laws derived from a Lyapunov function. The method drawback is the partially known machine model used for the design. Zhao et al. (2014) propose an adaptive flux observer to estimate stator and rotor resistances. However, uncertainties on inductances are not taken into account. Ouadi et al. (2002) and Accetta et al. (2016) use a magnetisation curve to estimate the value of the mutual inductance L_m . The disadvantage of this method is that this curve depends on the magnetising current. Therefore, it must be adjusted when the operating point changes. This estimation method is therefore not suitable for applications in which the speed changes frequently over a wide range. In Alonge et al. (2015), the authors present an estimation method for the rotor resistance and the mutual inductance but it does not take into account the uncertainties on stator and rotor inductances due to magnetic saturation. A model reference parameter identification algorithm is used to estimate the unknown inductances. Saad et al. (2019) and Yang et al. (2018) propose to estimate stator and rotor resistances and the mutual inductance. The rotor and stator inductances are assumed known and constant. The main drawback of the aforementioned works is that they consider either changes in resistances only, or changes in both resistances and mutual inductance. Stator and rotor inductances are assumed constant and known.

Several identification methods are proposed in the literature for the online estimation of induction machine parameters. These methods can be used in conjunction with conventional control methods for the design of robust and adaptive variable speed drive for induction machines. Indeed, Barut et al. (2011), Regaya et al. (2012) and Li et al. (2019) propose an online estimation for the rotor resistance only using an extended Kalman filter and fuzzy logic, respectively. Results show that the proposed algorithms do not guarantee a good estimate when the motor speed changes abruptly. Moreover, the stator resistance and motor inductances are assumed known and constant. Mapelli et al. (2017) propose to estimate the rotor resistance from the reactive power. The main drawback of the approach is that it is too sensitive to load torque changes. Huynh and Dunnigan (2012) propose a parameter estimation approach based on two advanced particle swarm optimisation algorithms. The proposed algorithms use experimental measurements of machine currents and active powers. Its main drawback is that it cannot be implemented in real-time. A neural network is proposed in Xu et al. (2019) and Bousserhane et al. (2006) for the design of a machine parameter identification algorithm. Only rotor and stator resistances are estimated. Inductances are assumed known and constant. It is worth mentioning that changes in the resistance and inductance values are caused by different physical phenomena. Indeed, it is the motor operating temperature that causes the change in the resistance values while the magnetic core saturation causes the change in

inductance values. Moreover, it is shown in Hinkkanen et al. (2006) and Fattah et al. (1999) that the magnetic core saturation in induction machines has a significant impact on stator and rotor inductances.

This paper assumes that all machine parameters namely rotor and stator resistances, stator, rotor and mutual inductances are unknown for the design of the variable speed drive for wound rotor induction motors. The design approach that is proposed uses a novel modelling approach for the induction machine in the $(\alpha\beta)$ reference frame. This model has two main advantages:

- 1 its state variables are constant in steady state
- 2 it has a triangular structure which enables the use of the backstepping control design technique.

The contribution of the paper is therefore an adaptive control for an induction machine assuming that rotor and stator resistances as well as stator, rotor and mutual inductance can change. A backstepping control design method is used to design the proposed variable speed control for induction machines. The result is a control structure in which a speed control is in series with a torque control in one side and a magnetic flux control is in series with a current control in the other side. An adaptation module is used to adjust the proposed controller parameters to ensure robust tracking performances in the presence of changes in machine resistances and inductances due to temperature and magnetic core saturation. The proposed controller is tested in simulation in the MATLAB/Simulink environment under various operating conditions.

The paper is organised as follows. Section 2 presents the novel model for induction machines. The model is used in Section 3 for the design of the proposed adaptive backstepping variable speed drive. The proposed controller is evaluated in Section 4. The paper ends with a conclusion.

2 Wound rotor induction motor model

The three-phase induction motor is the most widely used electric machine in the industry. Its operation and dynamic model are also well documented. This section presents the so-called energy model for the induction machine in which the state variables are stator and rotor currents. Note that the model can easily be obtained from the conventional induction machine model in which state variables are rotor and stator fluxes (Marino et al., 2010).

$$\frac{di_{s\alpha}}{dt} = -\frac{L_r R_s}{\Delta} i_{s\alpha} + \frac{MR_r}{\Delta} i_{r\alpha} + \frac{M^2 \omega}{\Delta} i_{s\beta} + \frac{ML_r \omega}{\Delta} i_{r\beta} + \frac{L_r}{\Delta} u_{s\alpha} \quad (1)$$

$$\frac{di_{s\beta}}{dt} = -\frac{L_r R_s}{\Delta} i_{s\beta} + \frac{MR_r}{\Delta} i_{r\beta} - \frac{M^2 \omega}{\Delta} i_{s\alpha} - \frac{ML_r \omega}{\Delta} i_{r\alpha} + \frac{L_r}{\Delta} u_{s\beta} \quad (2)$$

$$\frac{di_{r\alpha}}{dt} = -\frac{L_s R_r}{\Delta} i_{r\alpha} + \frac{MR_s}{\Delta} i_{s\alpha} - \frac{ML_s \omega}{\Delta} i_{s\beta} - \frac{L_s L_r \omega}{\Delta} i_{r\beta} - \frac{M}{\Delta} u_{s\alpha} \quad (3)$$

$$\frac{di_{r\beta}}{dt} = -\frac{L_s R_r}{\Delta} i_{r\beta} + \frac{MR_s}{\Delta} i_{s\beta} + \frac{ML_s \omega}{\Delta} i_{s\alpha} + \frac{L_s L_r \omega}{\Delta} i_{r\alpha} - \frac{M}{\Delta} u_{s\beta} \quad (4)$$

$$\frac{d\omega}{dt} = \frac{M}{J} (i_{s\beta} i_{r\alpha} - i_{s\alpha} i_{r\beta}) - \frac{T_L}{J} \quad (5)$$

with $\Delta = L_s L_r - M^2$.

$i_{s\alpha}$ and $i_{s\beta}$ are stator currents in the $\alpha\beta$ reference frame. $i_{r\alpha}$ and $i_{r\beta}$ are rotor currents in the $\alpha\beta$ axis reference frame. ω is the rotor speed in rad/s. T_L is the load torque N.m. J is the moment of inertia.

L_r , L_s and M : are respectively rotor, stator and mutual inductances. R_r and R_s are rotor and stator resistances.

Unlike the squirrel cage induction machine whose rotor windings are short-circuited and therefore not accessible, the rotor currents of the wound rotor induction machine are measurable. This machine is therefore suitable for the use of model-based nonlinear control design methods, which generally require that all system state variables be measurable. Indeed, these design methods require dynamic models whose state variables are constant in steady state. That is not the case for the energy model since its state variables are sinusoidal in steady state. This problem could easily be solved by transforming the state variables from the $(\alpha\beta)$ reference frame to the d/q reference frame. However, the main disadvantage of the d/q transformation is that it must be used in conjunction with its inverse transformation and both transformations are nonlinear and time varying. They require the rotor position and this considerably increases the computation required to perform the transformations. The following time invariant changes of variables are proposed in this paper instead. It consists of either equations (6) and (7) or equations (6) and (8).

$$\begin{cases} \Sigma = i_{r\alpha} i_{s\beta} - i_{r\beta} i_{s\alpha} \\ \Phi = i_{s\alpha} i_{r\alpha} + i_{s\beta} i_{r\beta} \end{cases} \quad (6)$$

$$\begin{cases} R = \frac{1}{2} (i_{r\beta}^2 + i_{r\alpha}^2) \\ \theta_R = a \tan \left(\frac{i_{r\beta}}{i_{r\alpha}} \right) \end{cases} \quad (7)$$

$$\begin{cases} S = \frac{1}{2} (i_{s\beta}^2 + i_{s\alpha}^2) \\ \theta_s = a \tan \left(\frac{i_{s\beta}}{i_{s\alpha}} \right) \end{cases} \quad (8)$$

The variable Σ is proportional to the electromagnetic torque. The variable Φ is the dot product between the stator and rotor currents. The physical meaning of this variable remains to be determined. The variable R is the square of

the RMS rotor current. The variable S is the square of the RMC stator current. These variables are constant when the machine is in steady state. θ_s is the angle of stator current and θ_r is the angle of rotor current. The proposed novel model for induction motor has the following equations:

$$\begin{aligned} \dot{\Sigma} = & -\frac{R_r L_s + R_s L_r}{\Delta} \Sigma - \frac{2ML_s \omega(t)}{\Delta} S - \frac{2ML_r \omega(t)}{\Delta} R \\ & - \frac{M^2 + L_s L_r}{\Delta} \omega(t) \Phi + \frac{M}{\Delta} (i_{s\alpha} u_{s\beta} - i_{s\beta} u_{s\alpha}) \\ & + \frac{L_r}{\Delta} (i_{r\alpha} u_{s\beta} - i_{r\beta} u_{s\alpha}) \end{aligned} \quad (9)$$

$$\begin{aligned} \dot{\Phi} = & -\frac{R_s L_r + R_r L_s}{\Delta} \Phi + \frac{2MR_r}{\Delta} R + \frac{2MR_s}{\Delta} S \\ & + \frac{M^2 + L_r L_s}{\Delta} \omega \Sigma + \frac{L_r}{\Delta} (i_{r\alpha} u_{s\alpha} + i_{r\beta} u_{s\beta}) \\ & - \frac{M}{\Delta} (i_{s\alpha} u_{s\alpha} + i_{s\beta} u_{s\beta}) \end{aligned} \quad (10)$$

$$\begin{aligned} \dot{R} = & -\frac{2R_r L_s}{\Delta} R - \frac{ML_s}{\Delta} \omega(t) \Sigma + \frac{R_s M}{\Delta} \Phi \\ & - \frac{M}{\Delta} (i_{r\alpha} u_{s\alpha} + i_{r\beta} u_{s\beta}) \end{aligned} \quad (11)$$

$$\begin{aligned} \dot{S} = & -\frac{2R_s L_r}{\Delta} S + \frac{R_r M}{\Delta} \Phi - \frac{ML_r}{\Delta} \omega(t) \Sigma \\ & + \frac{L_r}{\Delta} (i_{s\alpha} u_{s\alpha} + i_{s\beta} u_{s\beta}) \end{aligned} \quad (12)$$

$$\dot{\omega} = \frac{M}{J} \Sigma - \frac{T_L}{J} \quad (13)$$

Variables θ_s and θ_r are essential for the change of variables to be a diffeomorphism. They are not required for the design of the variable speed control therefore their dynamics are omitted for the sake of simplicity. The rotor flux (actually the square of the rotor flux) can be written in terms of the novel variables as follows.

$$\Psi_{2r} = 2L_r^2 R + 2L_r M \Phi + 2M^2 S \quad (14)$$

The following rotor flux dynamics are obtained by differentiating equation (14) and substituting equation (10), equation (11) and equation (12).

$$\dot{\Psi}_{2r} = -2MR_r \Phi - 4R_r L_r R \quad (15)$$

Moreover, if we define the following:

$$\Phi = \frac{1}{2L_r M} (\Psi_{2r} - 2L_r^2 R - 2M^2 S) \quad (16)$$

$$K = M^2 S - L_r^2 R \quad (17)$$

The rotor flux dynamics take the following form:

$$\dot{\Psi}_{2r} = -\frac{R_r}{L_r} \Psi_{2r} + \frac{2R_r}{L_r} K \quad (18)$$

A new variable K is defined and its dynamics have the following equation:

$$\begin{aligned} \dot{K} = & \frac{2R_r L_s L_r^2}{\Delta} R - \frac{2R_s L_r M^2}{\Delta} S \\ & + \left(\frac{R_r M^3}{\Delta} - \frac{R_s M L_r^2}{\Delta} \right) \\ & + \left(\frac{M L_s L_r^2}{\Delta} - \frac{M^3 L_r}{\Delta} \right) \omega(t) \Sigma \\ & + \frac{M^2 L_r}{\Delta} (i_{s\alpha} u_{s\alpha} + i_{s\beta} u_{s\beta}) \\ & + \frac{M L_r^2}{\Delta} (i_{r\alpha} u_{s\alpha} + i_{r\beta} u_{s\beta}) \end{aligned} \quad (19)$$

The dynamic equations necessary for the design of the novel adaptive variable speed control are given below. This model has a triangular form and therefore enables the utilisation of the recursive backstepping control design technique.

$$\dot{\omega} = \frac{M}{J} \Sigma - \frac{T_L}{J} \quad (20)$$

$$\begin{aligned} \dot{\Sigma} = & -\frac{R_r L_s + R_s L_r}{\Delta} \Sigma - \frac{2ML_s \omega(t)}{\Delta} S \\ & - \frac{2ML_r \omega(t)}{\Delta} R - \frac{M^2 + L_s L_r}{\Delta} \omega(t) \Phi \\ & + \frac{M}{\Delta} (i_{s\alpha} u_{s\beta} - i_{s\beta} u_{s\alpha}) + \frac{L_r}{\Delta} (i_{r\alpha} u_{s\beta} - i_{r\beta} u_{s\alpha}) \end{aligned} \quad (21)$$

$$\dot{\Psi}_{2r} = -\frac{R_r}{L_r} \Psi_{2r} + \frac{2R_r}{L_r} K \quad (22)$$

$$\begin{aligned} \dot{K} = & \frac{2R_r L_s L_r^2}{\Delta} R - \frac{2R_s L_r M^2}{\Delta} S \\ & + \left(\frac{R_r M^3}{\Delta} - \frac{R_s M L_r^2}{\Delta} \right) \Phi \\ & + \left(\frac{M L_s L_r^2}{\Delta} - \frac{M^3 L_r}{\Delta} \right) \omega(t) \Sigma \\ & + \frac{M^2 L_r}{\Delta} (i_{s\alpha} u_{s\alpha} + i_{s\beta} u_{s\beta}) \\ & + \frac{M L_r^2}{\Delta} (i_{r\alpha} u_{s\alpha} + i_{r\beta} u_{s\beta}) \end{aligned} \quad (23)$$

Next section presents a systematic design of the proposed adaptive variable speed drive for induction motors.

3 Adaptive backstepping control design

This section presents a new variable speed controller for wound rotor induction motors. The machine stator and rotor currents are measurable. However, machine parameters are assumed unknown, uncertain, or may change. These unknown parameters are machine resistances and inductances. The structure of the proposed control system as well as controller equations will be obtained from a recursive backstepping design approach. The main objective is to control the rotor speed and flux at their reference values despite the possible change in stator and rotor resistance and inductance values as well as the mutual

inductance value due to magnetic core saturation or to a change in machine operating temperature. A direct adaptive control design method will therefore be proposed to strengthen the robustness of the control structure against motor parameter changes. The adaptation module equations are derived from a stability study to ensure that the closed loop system remains stable.

3.1 Equations for the speed control loop

The equations for the speed control loop are presented in this section. The controller main task is to ensure that the motor speed tracks a speed reference value. A model based design strategy is proposed. Therefore, the dynamics of ω and Σ will be used to find the controller equations. For the sake of clarity, these dynamics are rewritten below:

$$\begin{cases} \dot{\omega} = p_1 \Sigma - p_2 \\ \dot{\Sigma} = -p_3 \Sigma - p_4 \omega(t) S \\ \quad - p_5 \omega(t) R - p_6 \omega(t) \Phi + p_7 v_1 + p_8 v_2 \end{cases} \quad (24)$$

where

$$p_1 = \frac{M}{J}; p_2 = \frac{T_L}{J}; p_3 = \frac{R_r L_s + R_s L_r}{\Delta}; p_4 = \frac{2ML_s}{\Delta};$$

$$p_5 = \frac{2ML_r}{\Delta}; p_6 = \frac{M^2 + L_s L_r}{\Delta}; p_7 = \frac{M}{\Delta}; p_8 = \frac{L_r}{\Delta}$$

$$v_1 = (i_{s\alpha} u_{s\beta} - i_{s\beta} u_{s\alpha}); v_2 = (i_{r\alpha} u_{s\beta} - i_{r\beta} u_{s\alpha})$$

The values for p_1, p_2, \dots, p_8 are unknown since machine parameters R_s, R_r, L_s, L_r and M are uncertain because they may change with operating conditions. An adaptive backstepping control design method is therefore used to find the controller equations along with the adaptation module that will adjust the controller parameters to ensure that the motor speed effectively tracks its reference despite uncertainties on the machine parameters. It is convenient to rewrite equation (24) into the following form that includes estimated model parameters ($\hat{p}_1, \hat{p}_2, \dots, \hat{p}_8$) and estimation errors ($\tilde{p}_1, \tilde{p}_2, \dots, \tilde{p}_8$) that are differences between true and estimated parameters.

$$\begin{cases} \dot{\omega} = \hat{p}_1 \Sigma - \hat{p}_2 + \tilde{p}_1 \Sigma - \tilde{p}_2 \\ \dot{\Sigma} = -\hat{p}_3 \Sigma - \hat{p}_4 \omega(t) S - \hat{p}_5 \omega(t) R \\ \quad - \hat{p}_6 \omega(t) \Phi + \hat{U}_1 - \tilde{p}_3 \Sigma - \tilde{p}_4 \omega(t) S \\ \quad - \tilde{p}_5 \omega(t) R - \tilde{p}_6 \omega(t) \Phi + \tilde{p}_7 v_1 + \tilde{p}_8 v_2 \end{cases} \quad (25)$$

where $\hat{U}_1 = \hat{p}_7 v_1 + \hat{p}_8 v_2$.

The design procedure is now presented. The following variable which is the speed error is defined first.

$$\tilde{\omega} = \omega - \omega_{ref} \quad (26)$$

ω_{ref} is the reference value for the mechanical speed. The speed error dynamics are easily obtained by differentiating equation (26). For the sake of simplicity, it is assumed that

the speed reference value is constant therefore its derivative is zero.

$$\dot{\tilde{\omega}} = \hat{p}_1 \Sigma - \hat{p}_2 + \tilde{p}_1 \Sigma - \tilde{p}_2 \quad (27)$$

Equation (27) is used to find the value that the variable Σ should have to make the speed error converge to zero. This desired value for the variable Σ has the following expression:

$$\Sigma^* = \frac{1}{\hat{p}_1} (\hat{p}_2 - k_1 \tilde{\omega}) \quad (28)$$

The gain k_1 is a positive number. Note that equation (28) depends on estimated parameters that are provided by an adaptation module whose equations are yet to be determined. Σ^* is used to define the following new variable that represents the error between Σ and its reference Σ^* .

$$\tilde{\Sigma} = \Sigma - \Sigma^* \quad (28)$$

The speed error dynamics can be rewritten in terms of the new variables defined above. The equation will be used to verify the closed loop stability of the system.

$$\dot{\tilde{\omega}} = \hat{p}_1 \tilde{\Sigma} - k_1 \tilde{\omega} + \tilde{p}_1 \Sigma - \tilde{p}_2 \quad (29)$$

Next, the expression for \hat{U}_1 that will guarantee that the variable Σ will converge to its desired value is now obtained. This requires the dynamics for $\tilde{\Sigma}$ which are easily obtained by differentiating equation (29) and substituting equation (25).

$$\begin{aligned} \dot{\tilde{\Sigma}} &= \dot{\Sigma} - \dot{\Sigma}^* \\ &= -\hat{p}_3 \Sigma - \hat{p}_4 \omega(t) S - \hat{p}_5 \omega(t) R - \hat{p}_6 \omega(t) \Phi + \hat{U}_1 \\ &\quad - \tilde{p}_3 \Sigma - \tilde{p}_4 \omega(t) S - \tilde{p}_5 \omega(t) R - \tilde{p}_6 \omega(t) \Phi \\ &\quad + \tilde{p}_7 v_1 + \tilde{p}_8 v_2 - \frac{\dot{\hat{p}}_2}{\hat{p}_1} + \frac{k_1}{\hat{p}_1} (\hat{p}_1 \Sigma - \hat{p}_2) \\ &\quad + \frac{k_1}{\hat{p}_1} (\tilde{p}_1 \Sigma - \tilde{p}_2) + \frac{\dot{\hat{p}}_1}{\hat{p}_1^2} (\hat{p}_2 - k_1 \tilde{\omega}) \end{aligned} \quad (30)$$

The following expression is proposed for \hat{U}_1 . One can note that it depends on estimated parameters that are provided by the adaptation module. The gain k_2 is a positive number. It's worth mentioning that \hat{U}_1 will be used to find the true controller output signals later.

$$\begin{aligned} \hat{U}_1 &= \hat{p}_3 \Sigma + \hat{p}_4 \omega(t) S + \hat{p}_5 \omega(t) R + \hat{p}_6 \omega(t) \Phi \\ &\quad + \frac{\dot{\hat{p}}_2}{\hat{p}_1} + k_1 \left(-\Sigma + \frac{\hat{p}_2}{\hat{p}_1} \right) - \frac{\dot{\hat{p}}_1}{\hat{p}_1^2} (\hat{p}_2 - k_1 \tilde{\omega}) - k_2 \tilde{\Sigma} - \hat{p}_1 \tilde{\omega} \end{aligned} \quad (31)$$

Substituting equation (32) into equation (31) yields the following dynamics that will be used to assess the closed loop stability of the system.

$$\begin{aligned} \dot{\tilde{\Sigma}} &= -\tilde{p}_3 \Sigma - \tilde{p}_4 \omega(t) S - \tilde{p}_5 \omega(t) R - \tilde{p}_6 \omega(t) \Phi \\ &\quad + \tilde{p}_7 v_1 + \tilde{p}_8 v_2 + \frac{k_1}{\hat{p}_1} (\tilde{p}_1 \Sigma - \tilde{p}_2) - k_2 \tilde{\Sigma} - \hat{p}_1 \tilde{\omega} \end{aligned} \quad (32)$$

The adaptation module equations are now presented in the next paragraph. These equations are normally derived from the closed loop stability of the system. However, for the sake of simplicity, the result of this stability study is shown first and the stability is verified later. The following equations represent the adaptation laws. They are the estimated parameter dynamics and are used to adjust the controller parameters so that the speed error and $\tilde{\Sigma}$ converge to zero despite that machine parameters are unknown.

$$\dot{\hat{p}}_1 = \gamma_1 \left(-\tilde{\omega}\Sigma - \frac{k_1}{\hat{p}_1} \tilde{\Sigma} \right) \quad (33)$$

$$\dot{\hat{p}}_2 = -\gamma_2 \left(\tilde{\omega} - \frac{k_1}{\hat{p}_1} \tilde{\Sigma} \right) \quad (34)$$

$$\dot{\hat{p}}_3 = \gamma_3 (\Sigma \tilde{\Sigma}) \quad (35)$$

$$\dot{\hat{p}}_4 = \gamma_4 (-\omega S \tilde{\Sigma}) \quad (36)$$

$$\dot{\hat{p}}_5 = \gamma_5 (-\omega R \tilde{\Sigma}) \quad (37)$$

$$\dot{\hat{p}}_6 = \gamma_6 (-\omega \Phi \tilde{\Sigma}) \quad (38)$$

$$\dot{\hat{p}}_7 = \gamma_7 (v_1 \tilde{\Sigma}) \quad (39)$$

$$\dot{\hat{p}}_8 = \gamma_8 (v_2 \tilde{\Sigma}) \quad (40)$$

Parameters $\gamma_1, \gamma_2, \dots, \gamma_8$ are positive adaptation gains that are selected by the designer.

3.2 Equations for the flux control loop

The objective in this section is to find the flux control loop equations. This controller ensures that the motor flux remains constant or tracks a reference value. Dynamics that are used for the design are rewritten below.

$$\begin{cases} \dot{\Psi}_{2r} = -\theta_1 \Psi_{2r} + 2\theta_1 K \\ \dot{K} = \theta_3 R - \theta_4 S + \theta_5 \Phi + \theta_6 \omega(t) \Sigma + \theta_7 v_3 + \theta_8 v_4 \end{cases} \quad (41)$$

with

$$v_3 = (i_{s\alpha} u_{s\alpha} + i_{s\beta} u_{s\beta}); v_4 = (i_{r\alpha} u_{s\alpha} + i_{r\beta} u_{s\beta});$$

$$\theta_1 = \frac{R_r}{L_r}; \theta_3 = \frac{2R_r L_s L_r^2}{\Delta}; \theta_4 = \frac{2R_s L_r M^2}{\Delta};$$

$$\theta_5 = \frac{R_r M^3 - R_s M L_r^2}{\Delta}; \theta_6 = \frac{M L_s L_r^2 - M^3 L_r}{\Delta};$$

$$\theta_7 = \frac{M^2 L_r}{\Delta}; \theta_8 = \frac{M L_r^2}{\Delta}$$

Parameters $\theta_1, \theta_2, \dots, \theta_8$ are unknown since they depends on unknown machine parameters R_s, R_r, L_s, L_r and M . An adaptive backstepping control design approach is used to find the controller equation. Equation (42) is rewritten in terms of estimated model parameters $(\hat{\theta}_1, \hat{\theta}_2, \dots, \hat{\theta}_8)$ and estimation errors $(\tilde{\theta}_1, \tilde{\theta}_2, \dots, \tilde{\theta}_8)$ as follows:

$$\begin{cases} \dot{\Psi}_{2r} = -\hat{\theta}_1 \Psi_{2r} + 2\hat{\theta}_1 K - \tilde{\theta}_1 \Psi_{2r} + 2\tilde{\theta}_1 K \\ \dot{K} = \hat{\theta}_3 R - \hat{\theta}_4 S + \hat{\theta}_5 \Phi + \hat{\theta}_6 \omega(t) \Sigma + \hat{U}_2 \\ \quad + \tilde{\theta}_3 R - \tilde{\theta}_4 S + \tilde{\theta}_5 \Phi + \tilde{\theta}_6 \omega(t) \Sigma + \tilde{\theta}_7 v_3 + \tilde{\theta}_8 v_4 \end{cases} \quad (43)$$

where $\hat{U}_2 = \hat{\theta}_7 v_3 + \hat{\theta}_8 v_4$.

Next paragraph presents the step by step design procedure. The following variable which is the flux error is defined first.

$$\tilde{\Psi}_{2r} = \Psi_{2r} - \Psi_{2rref} \quad (44)$$

Ψ_{2rref} is the reference value for the flux rotor. The flux error dynamics are obtained by differentiating equation (44). It is assumed that the flux reference value is constant for the sake of simplicity. The dynamics have the following expression:

$$\dot{\tilde{\Psi}}_{2r} = -\hat{\theta}_1 \Psi_{2r} + 2\hat{\theta}_1 K - \tilde{\theta}_1 \Psi_{2r} + 2\tilde{\theta}_1 K \quad (45)$$

Equation (45) is used to find the value that the variable K must have to make Ψ_{2r} converge to zero. This value is denoted K^* and it has the following expression:

$$K^* = \frac{1}{2\hat{\theta}_1} (\hat{\theta}_1 \Psi_{2r} - k_3 \tilde{\Psi}_{2r}) \quad (46)$$

The gain k_3 is a positive number. Note that equation (46) depends on estimated parameters coming from an adaptation module yet to be designed. K^* is used to define the following new variable which represents the error between K and its reference K^* .

$$\tilde{K} = K - K^* \quad (47)$$

The flux error dynamics can be rewritten in terms of the new variables defined above. Equation (48) will be used to verify the closed loop stability of the system.

$$\dot{\tilde{\Psi}}_{2r} = 2\hat{\theta}_1 \tilde{K} - k_3 \tilde{\Psi}_{2r} - \tilde{\theta}_1 \Psi_{2r} + 2\tilde{\theta}_1 K \quad (48)$$

Next, the expression for \hat{U}_2 that will guarantee that the variable K will converge to its desired value is now obtained. This requires the dynamics for \tilde{K} which is easily obtained by differentiating equation (47) and substituting equation (42).

$$\begin{aligned}
\dot{\tilde{K}} &= \hat{\theta}_3 R - \hat{\theta}_4 S + \hat{\theta}_5 \Phi + \hat{\theta}_6 \omega(t) \Sigma + \hat{U}_2 \\
&+ \tilde{\theta}_3 R - \tilde{\theta}_4 S + \tilde{\theta}_5 \Phi + \tilde{\theta}_6 \omega(t) \Sigma + \tilde{\theta}_7 v_3 + \tilde{\theta}_8 v_4 \\
&- \frac{\dot{\hat{\theta}}_1}{2\hat{\theta}_1} \Psi_{2r} - \frac{1}{2\hat{\theta}_1} (\hat{\theta}_1 - k_3) (\hat{\theta}_1 \Psi_{2r} + 2\hat{\theta}_1 K) \\
&- \frac{1}{2\hat{\theta}_1} (\hat{\theta}_1 - k_3) (\tilde{\theta}_1 \Psi_{2r} + 2\tilde{\theta}_1 K) \\
&+ \frac{\dot{\hat{\theta}}_1}{2\hat{\theta}_1} (\hat{\theta}_1 \Psi_{2r} - k_3 \tilde{\Psi}_{2r})
\end{aligned} \quad (49)$$

The following expression is proposed for \hat{U}_2 . One can note that it depends on estimated parameters that are provided by the adaptation module. The gain k_4 is a positive real number.

$$\begin{aligned}
\hat{U}_2 &= -\hat{\theta}_3 R + \hat{\theta}_4 S - \hat{\theta}_5 \Phi - \hat{\theta}_6 \omega(t) \Sigma \\
&- \frac{\dot{\hat{\theta}}_1}{2\hat{\theta}_1^2} (\hat{\theta}_1 \Psi_{2r} - k_3 \tilde{\Psi}_{2r}) + \frac{\dot{\hat{\theta}}_1}{2\hat{\theta}_1} \Psi_{2r} \\
&+ \frac{1}{2} (\hat{\theta}_1 - k_3) (\Psi_{2r} - 2K) - 2\hat{\theta}_1 \tilde{\Psi}_{2r} - k_4 \tilde{K}
\end{aligned} \quad (50)$$

Substituting equation (50) into equation (49) yields the following dynamics that will be used to assess the closed loop stability of the system.

$$\begin{aligned}
\dot{\tilde{K}} &= -\frac{1}{2\hat{\theta}_1} (\hat{\theta}_1 - k_3) (\tilde{\theta}_1 \Psi_{2r} + 2\tilde{\theta}_1 K) + \tilde{\theta}_3 R - \tilde{\theta}_4 S \\
&+ \tilde{\theta}_5 \Phi + \tilde{\theta}_6 \omega(t) \Sigma + \tilde{\theta}_7 v_3 + \tilde{\theta}_8 v_4 - 2\hat{\theta}_1 \tilde{\Psi}_{2r} - k_4 \tilde{K}
\end{aligned} \quad (51)$$

Estimated parameters that appear in equations (46) and (50) are obtained from the following adaptation laws:

$$\dot{\hat{\theta}}_1 = \delta_1 \left[\tilde{\Psi}_{2r} (-\Psi_{2r} + 2K) - \tilde{K} \left(\frac{1}{2\hat{\theta}_1} (\Psi_{2r} + 2K) \right) \right] \quad (52)$$

$$\dot{\hat{\theta}}_3 = \delta_3 \tilde{\Psi}_{2r} R \quad (53)$$

$$\dot{\hat{\theta}}_4 = -\delta_4 \tilde{\Psi}_{2r} S \quad (54)$$

$$\dot{\hat{\theta}}_5 = \delta_5 \tilde{\Psi}_{2r} \Phi \quad (55)$$

$$\dot{\hat{\theta}}_6 = \delta_6 \tilde{\Psi}_{2r} \omega(t) \Sigma \quad (56)$$

$$\dot{\hat{\theta}}_7 = \delta_7 \tilde{\Psi}_{2r} v_3 \quad (57)$$

$$\dot{\hat{\theta}}_8 = \delta_8 \tilde{\Psi}_{2r} v_4 \quad (58)$$

Parameters $\delta_1, \delta_3, \dots, \delta_8$ are positive adaptation gains that are selected by the designer. These equations are derived from the closed loop stability of the system. The stability study is presented later. Next paragraph shows how the stator voltages u_{sa} and u_{sb} are computed from equations (32) and (50). Indeed, U_1 and U_2 , in terms of estimated parameters, stator and rotor currents and stator voltages are as follows:

$$\begin{cases} \hat{U}_1 = \hat{p}_7 (i_{s\alpha} u_{s\beta} - i_{s\beta} u_{s\alpha}) + \hat{p}_8 (i_{r\alpha} u_{s\beta} - i_{r\beta} u_{s\alpha}) \\ \hat{U}_2 = \hat{\theta}_7 (i_{s\alpha} u_{s\beta} + i_{s\beta} u_{s\alpha}) + \hat{\theta}_8 (i_{r\alpha} u_{s\beta} + i_{r\beta} u_{s\alpha}) \end{cases} \quad (59)$$

Stator voltages that are the controller output signals have the followings expressions therefore

$$\begin{bmatrix} u_{s\alpha} \\ u_{s\beta} \end{bmatrix} = \begin{bmatrix} (-\hat{p}_7 i_{s\alpha} - \hat{p}_8 i_{r\beta}) & (\hat{p}_7 i_{s\alpha} + \hat{p}_8 i_{r\alpha}) \\ (\hat{\theta}_7 i_{s\beta} + \hat{\theta}_8 i_{r\alpha}) & (\hat{\theta}_7 i_{s\beta} + \hat{p}_8 i_{r\beta}) \end{bmatrix}^{-1} \begin{bmatrix} \hat{U}_1 \\ \hat{U}_2 \end{bmatrix} \quad (60)$$

The matrix that appears in equation (60) is invertible when the machine is in normal operation mode and estimated parameters are kept away from zero. Indeed the matrix determinant has the following form:

$$\Lambda = -2\hat{p}_7 \hat{\theta}_7 S - 2\hat{p}_8 \hat{\theta}_8 R - (\hat{p}_8 \hat{\theta}_7 + \hat{p}_7 \hat{\theta}_8) \Phi$$

In normal operation, variables R, S and Φ are not zero. Estimated parameters can easily be forced to remain within a predefined domain using a projection method not discussed in the paper for the sake of simplicity.

Figure 1 summarises the control structure that results from the proposed design approach. It has two control loops: the speed and flux control loops. The speed control loop consists of two sub-controllers in series: The speed controller represented by equation (28) and the torque controller given by equation (32). The speed controller provides the reference signal for the torque controller. The flux control loop has two controllers in series: The flux controller represented by equation (46) followed by a current controller described by equation (50). The flux controller provides the reference signal for the current control. The proposed control structure also includes two adaptation modules which are used to adjust the controller parameters when motor parameters change. Although the proposed control structure looks very similar to conventional control structures for asynchronous motors, it has the advantage that it is not only nonlinear but also adaptive. Moreover, it guarantees that the system is stable and that the speed and flux always converge to their desired values although motor resistances and inductances are subject to changes.

Figure 1 The proposed control structure

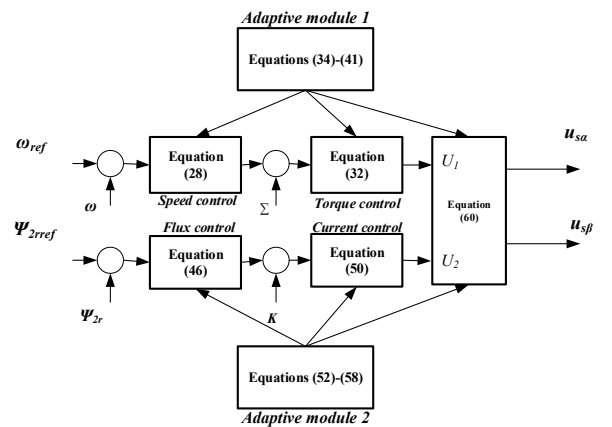
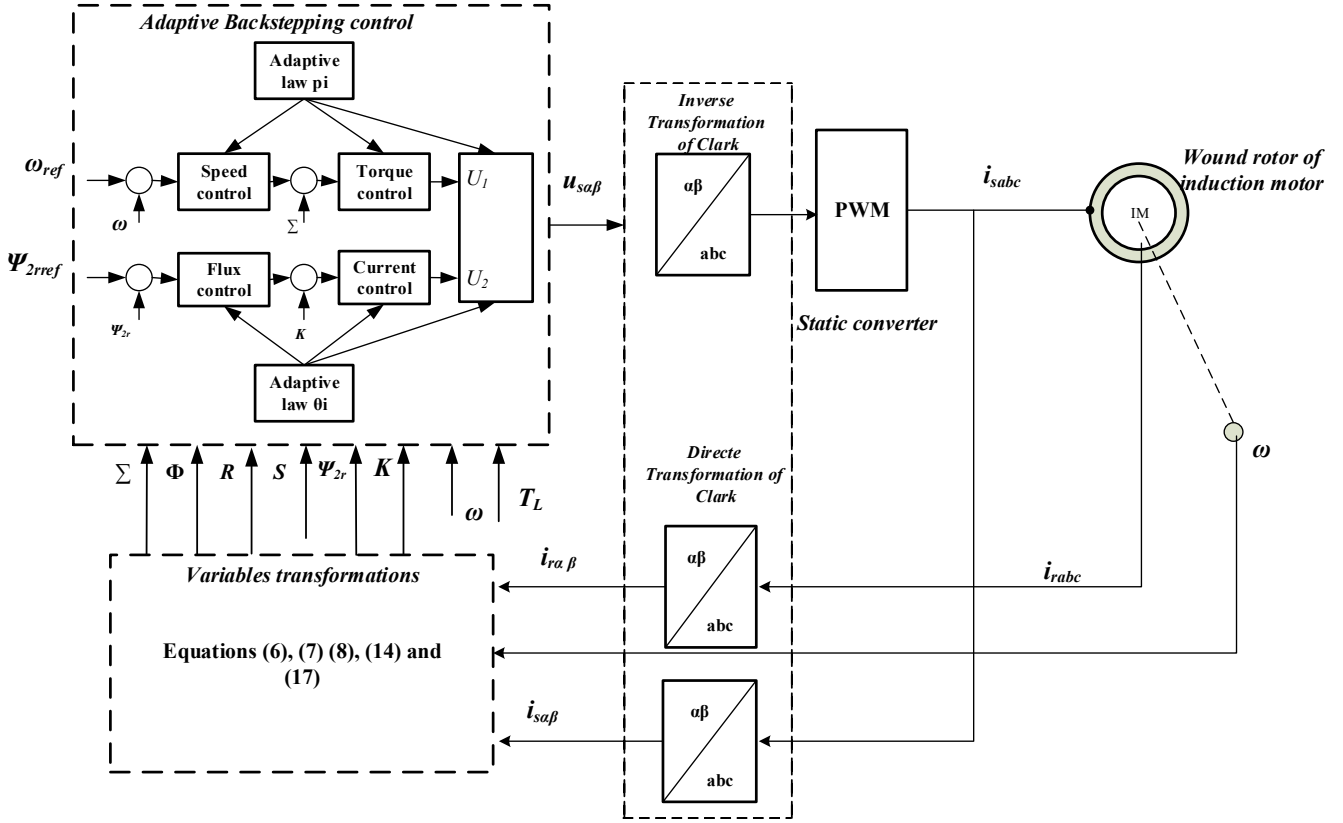


Figure 2 The proposed variable speed control structure (see online version for colours)



3.3 Stability analysis

The stability analysis is done in this section using the Lyapunov method. We define the following Lyapunov candidate function therefore

$$V = \frac{1}{2}(\tilde{\omega}^2 + \tilde{\Sigma}^2 + \tilde{\Psi}_{2r}^2 + \tilde{K}^2) + \frac{1}{2} \sum_{i=1}^8 \frac{1}{\gamma_i} \tilde{p}_i^2 + \frac{1}{2} \sum_{i=1}^8 \frac{1}{\delta_i} \tilde{\theta}_i^2 \quad (61)$$

V is differentiated and equation (62) is obtained

$$\dot{V} = \tilde{\omega}\dot{\tilde{\omega}} + \tilde{\Sigma}\dot{\tilde{\Sigma}} + \tilde{\Psi}_{2r}\dot{\tilde{\Psi}_{2r}} + \tilde{K}\dot{\tilde{K}} - \sum_{i=1}^8 \frac{1}{\gamma_i} \tilde{p}_i\dot{\tilde{p}}_i - \sum_{i=1}^8 \frac{1}{\delta_i} \tilde{\theta}_i\dot{\tilde{\theta}}_i \quad (62)$$

Substituting equations (30), (33), (48) and (51) in equation (62) we have:

$$\dot{V} = -k_1\tilde{\omega}^2 - k_2\tilde{\Sigma}^2 - k_3\tilde{\Psi}_{2r}^2 - k_4\tilde{K}^2 \quad (63)$$

$\dot{V} \leq 0$ for all $k_i \geq 0 \{i = 1, 2, 3, 4\}$. The system is therefore stable. Next paragraph shows that the motor speed and the rotor flux converge towards their reference values. The objective is to show that $\tilde{\omega}$, $\tilde{\Sigma}$, $\tilde{\Psi}_{2r}$, \tilde{K} converge to zero as time goes to infinity.

Indeed, $V(t) < V(0)$ since $V(t)$ is a decreasing function. Moreover $\tilde{\omega}$, $\tilde{\Sigma}$, $\tilde{\Psi}_{2r}$, \tilde{K} are bounded since the system is stable. In addition,

$$\ddot{V} = -2k_1\tilde{\omega}\dot{\tilde{\omega}} - 2k_2\tilde{\Sigma}\dot{\tilde{\Sigma}} - 2k_3\tilde{\Psi}_{2r}\dot{\tilde{\Psi}_{2r}} - 2k_4\tilde{K}\dot{\tilde{K}} \quad (64)$$

$\ddot{V}(t)$ is bounded therefore $V(t)$ is uniformly bounded. By the Barbalat lemma $\tilde{\omega}$, $\tilde{\Sigma}$, $\tilde{\Psi}_{2r}$, \tilde{K} converge to zero as time goes to infinity.

3.4 The proposed variable speed drive

Figure 2 shows the proposed control system for the wound rotor induction motor. The three-phase stator and rotor currents as well as the speed of the motor are measured. The α/β components of the currents are then obtained using two Clark transformation modules. Then, the proposed change of variables is performed. The new variables and motor speed are used in the adaptive backstepping control module to compute the controller output signals. These signals are converted back to the three-phase ABC reference frame using the Clark transformation module and applied to the PWM that is connected to the motor. The outputs of this inverter are applied to the motor stator.

4 Simulation and results

The proposed adaptive variable speed control is evaluated in this section. Several simulations were carried out under different operating conditions. This includes a starting-up at rated load, load changes, and speed and flux reference changes. Machine resistances and inductances change during each of the test conditions. The rated parameter values for the wound rotor induction motor are as follows: $R_s = 5.3 \Omega$, $R_r = 3.3 \Omega$, $L_s = 0.365 \text{ H}$, $L_r = 0.375 \text{ H}$,

$L_m = 0.34$ H and $J = 0.0075$ kg.m² the rated load torque is $T_L = 5$ N. The maximum stator voltage is 700V. Controller gains are $k_1 = 180$, $k_2 = 80$, $k_3 = 930$ and $k_4 = 1,245$. Adaptation law gains are set to zero except for $\gamma_3 = 5.5$ and $\delta_3 = 5.67$. In the first test, the motor operates in an overspeed condition. The objective of this test 1 is to evaluate the performance of the proposed controller in tracking the rotating speed and rotor flux references.

Note that the machine resistances and inductances change during this test as illustrated in Figures 3 and 4. The stator and rotor resistances R_s and R_r generally change with the temperature. We have therefore assumed that the increases of 63.77% for R_s and 68.03% for R_r occur simultaneously with the increase in load torque. At start-up, the load torque is 2.5 Nm and it increases to 5.8 Nm at 2.5 s as shown in Figure 6.

When operating in the overspeed condition, the rotor flux reference is reduced (as illustrated in Figure 5) to limit the machine input voltage. This is referred to as Field weakening. The resulting decrease in rotor flux will induce an increase in stator, rotor and mutual inductances due to the magnetic core saturation. In our test, this increase in inductances is 13.7% for L_s , 13.3% for L_r and 14.7% for L_m . At $t = 5$ s, the speed is increased up to 10% of its rated value as shown in Figure 7 and the rotor flux is reduced by 21.2% as illustrated in Figure 5. Figure 6 shows a good transient response for the motor torque. The controller does not induce some ripples in the torque as it is the case in certain works in the literature (Saad et al., 2019). In Figure 7, the speed reference ω_{ref} is increased from 104.5 rad/s to 115 rad/s between 5 s and 6.5 s. We observe that the motor rotation speed follows its reference speed ω_{ref} despite changes in the motor parameters. At $t = 2.5$ s during the change in resistances R_s and R_r , a slight increase in ω_r compared to ω_{ref} is observed but the speed quickly returns to its reference value. The controller is therefore robust in the presence of changes in R_r and R_s . Also, at $t = 5$ s, the inductances L_s , L_r and L_m change. The motor speed increases slightly and quickly return to its reference value. The speed control is also robust against changes in inductances due to saturation of the magnetic flux. In Figure 8, we observe that the flux reference is reduced from its rated value of 1.16 Wb to 0.98 Wb to limit the voltage at the inverter terminals while maintaining the maximum torque. The resulting reduction in flux will cause inductances L_s , L_r and L_m to increase. It is observed that the flux Ψ_{2r} follows its reference Ψ_{2rref} with a slight error in steady state although the parameters L_s , L_r and L_m change. This result confirms that the controller is robust. Controller parameters θ_3 and θ_6 are illustrated respectively in Figures 18 and 19. We can see that they remain bounded.

Figures 10, 11, 12, 13 and 14, respectively illustrate the variables Σ , Φ , R , S and K of the proposed new model for induction motors. It is observed that these signals are constant in steady state. The proposed model is in the (α/β) reference frame however it has the same advantage as the traditional model in the (dq) reference frame for the design of nonlinear controllers. Contrary to the traditional model the new model does not require the electrical angle θ_s . Figure 15 shows the stator current. It is observed that it increases when the load increases. At $t = 2.5$ s, the increase in the load torque to 5.8 N.m (see Figure 6) causes an increase in the stator current to its nominal value of 4.5 A. Figures 16, 17, 18 and 19 show the controller parameters. We see that these parameters are bounded. The main objective of the second test is to assess the effectiveness of the proposed controller when the machine starts at its rated load, the speed deceleration and the change in the rotation direction in the presence of changes in machine resistances and inductances. Figure 20 shows the rotor speed. One can observe that the speed tracks its reference value with a steady-state error close to zero. In addition, at $t = 2.5$ s, R_s and R_r increase respectively to 63% and 68% of their rated values respectively. The system remains stable. The tracking error remains negligible. We can also observe an increase in the inverter terminal voltage when R_r and R_s change. The system remains stable during the deceleration and change in rotation direction. However, during this change, we observe that the electric torque T_e (see Figure 24) drops during 0.5 s and then returns to its initial value. Figure 21 shows that the rotor flux increases from its rated value of 1.16 wb to the value of 1.24 wb. This increase leads to a reduction of the inductances L_s , L_r and L_m due to the magnetic core saturation. A peak of increase in the rotor flux is observed then the flux perfectly tracks its reference Ψ_{2rref} . Figure 24 shows that the stator current returns to its rated value after a change of the machine rotation direction.

Figure 3 Stator and rotor resistance change profiles

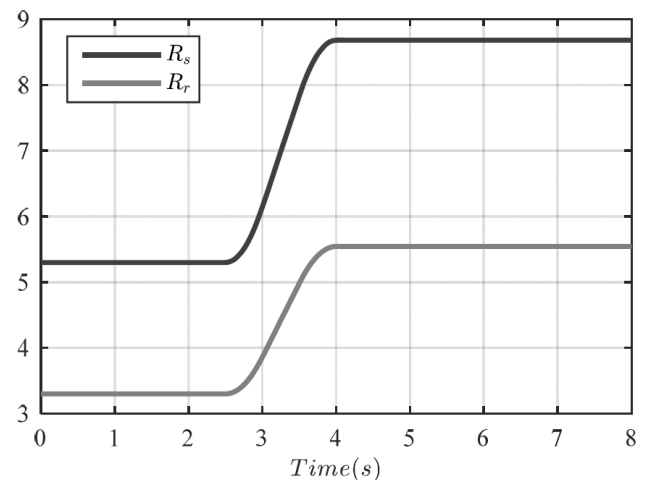


Figure 4 Inductance change profiles

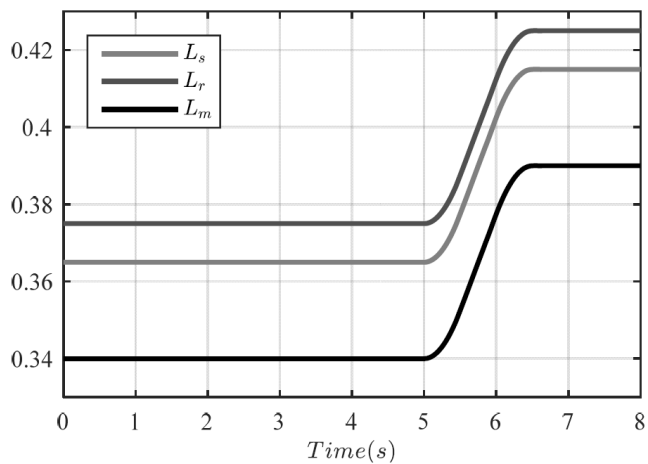


Figure 5 Flux reference change profile

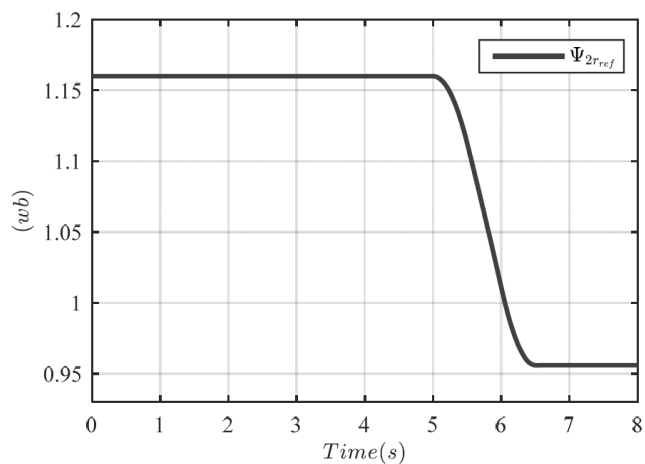


Figure 6 Load torque and electric torque waveforms

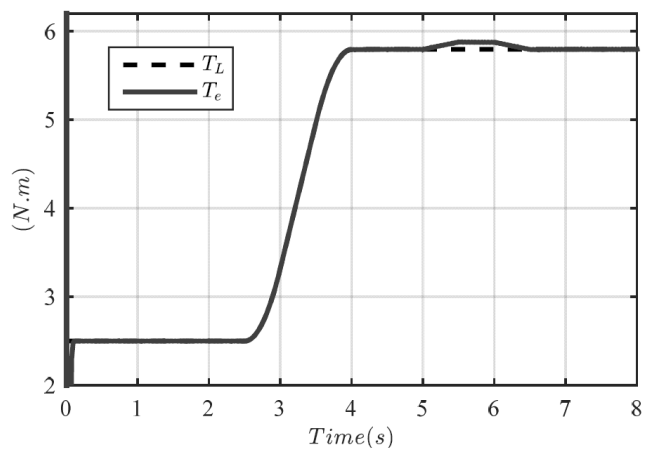


Figure 7 Rotor speed waveform

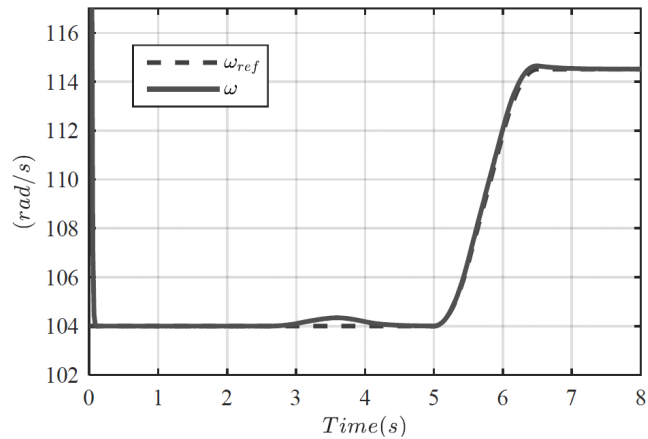


Figure 8 Rotor flux waveform

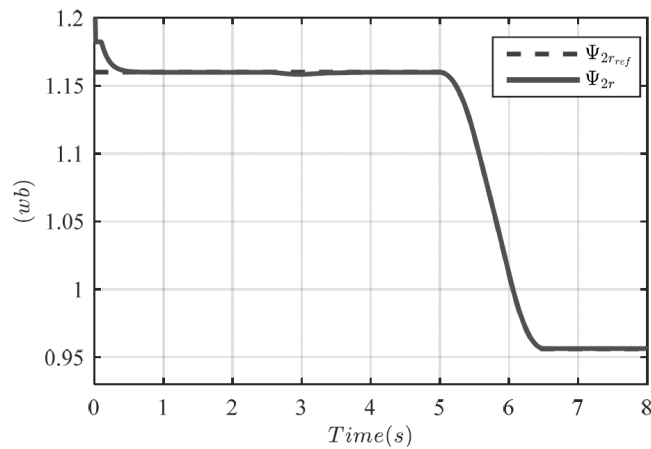


Figure 9 Stator voltage amplitude

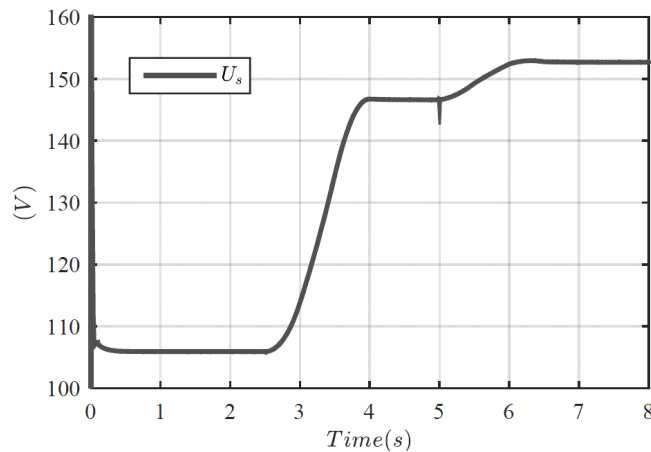


Figure 10 Variable Σ waveform

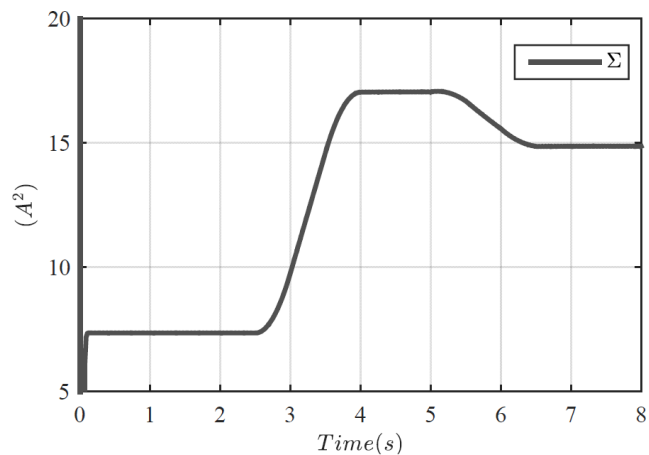


Figure 13 Variable S waveform

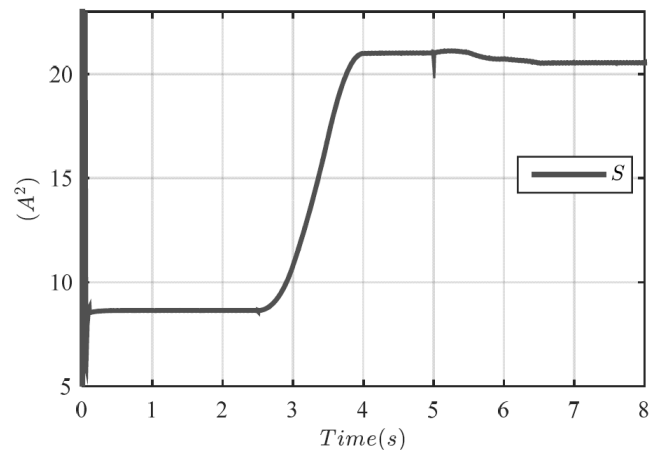


Figure 11 Variable Φ waveform

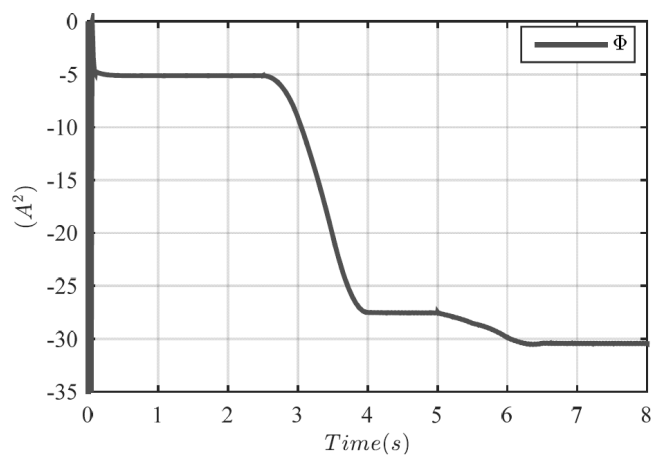


Figure 14 Variable K waveform

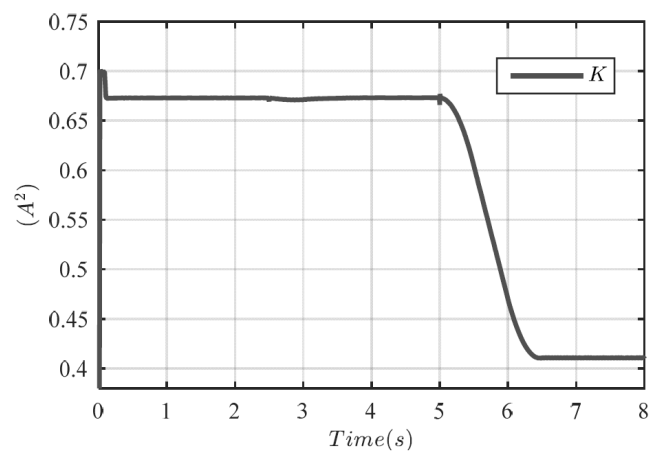


Figure 12 Variable R waveform

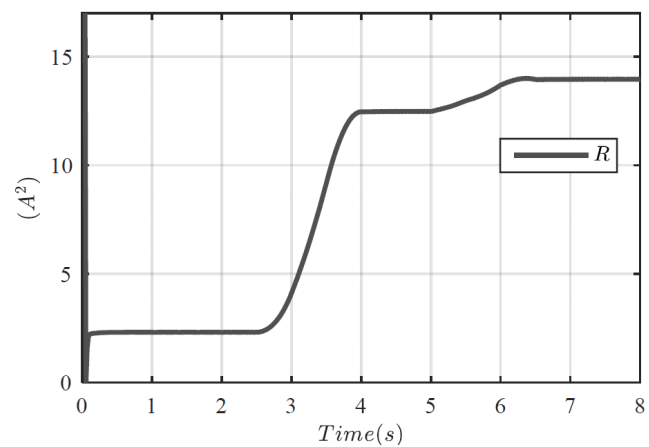


Figure 15 Stator current waveform (see online version for colours)

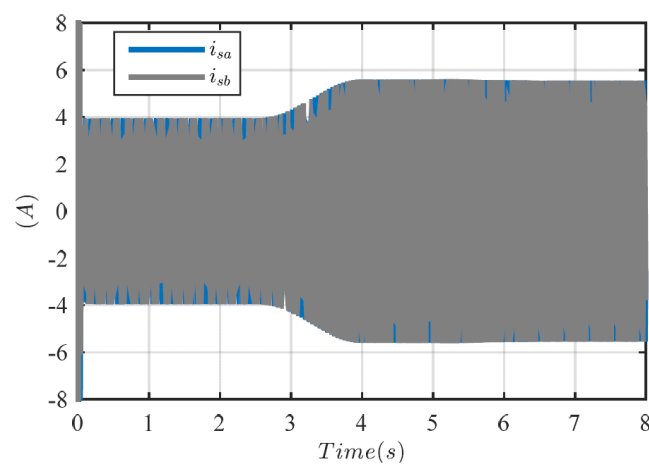


Figure 16 Estimated parameter p_1

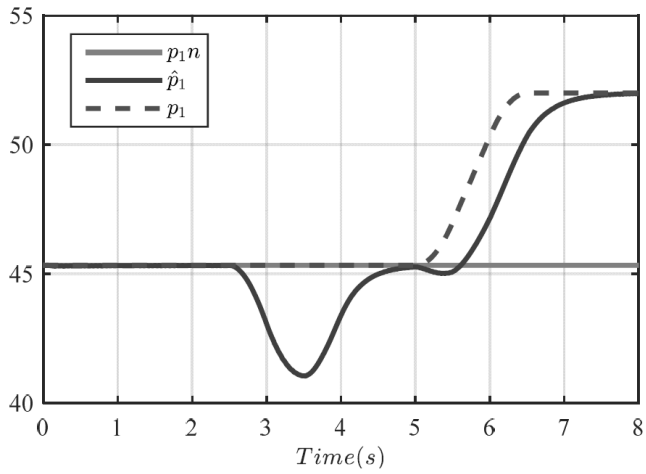


Figure 19 Estimated parameter θ_6

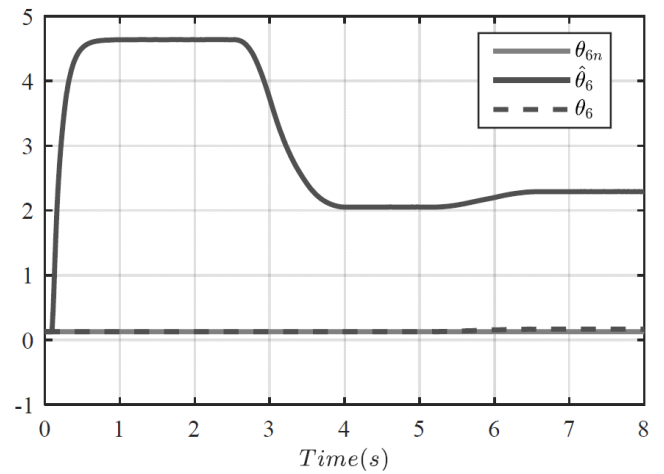


Figure 17 Estimated parameter p_3

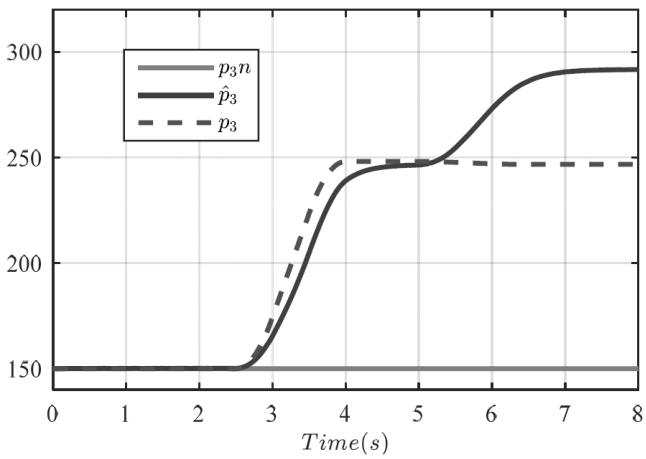


Figure 20 Rotor speed during test 2

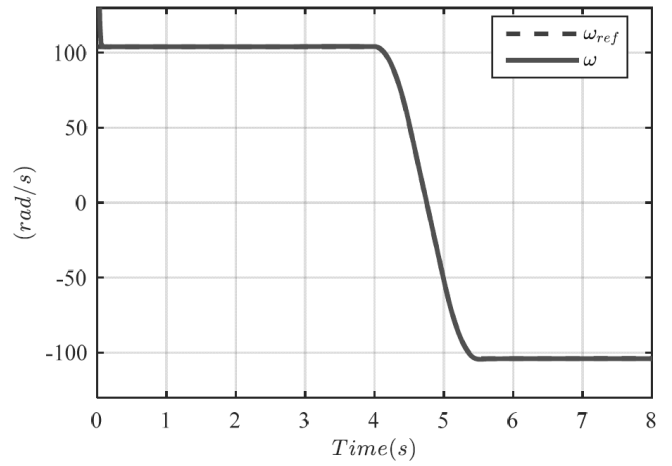


Figure 18 Estimated parameter θ_3

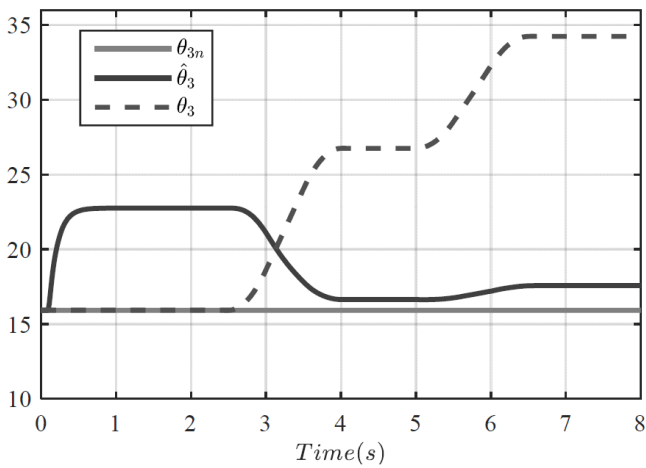


Figure 21 Rotor flux during test 2

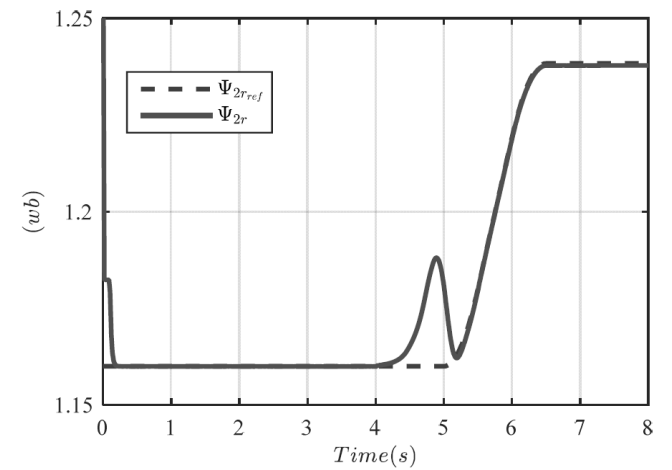


Figure 22 Stator voltage during test 2

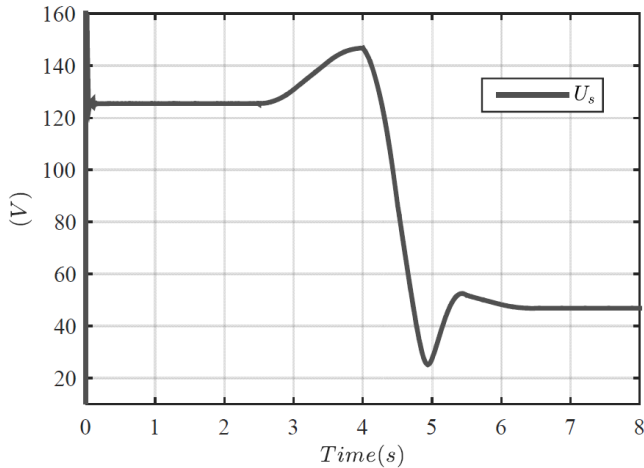


Figure 23 Load torque and electric torque during test 2

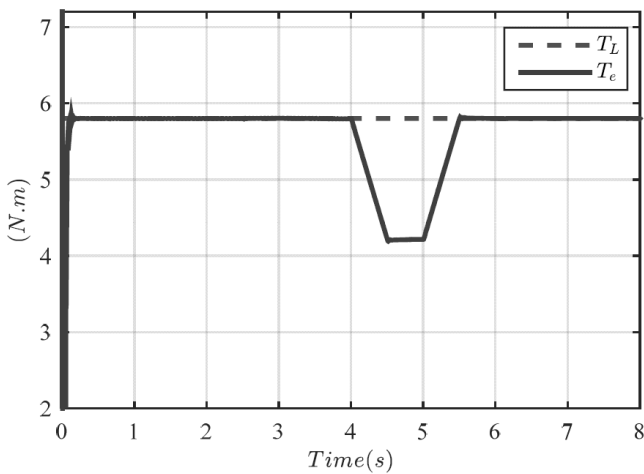
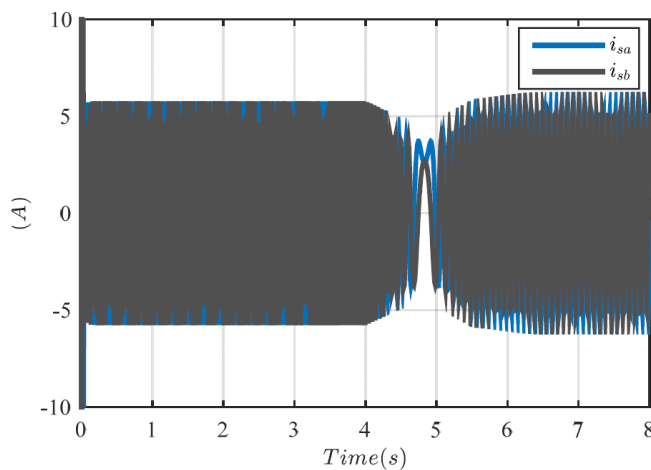


Figure 24 Stator current during test 2 (see online version for colours)



5 Conclusions

In this paper, an adaptive backstepping control is proposed for the design of a variable speed control for induction motors. We have proposed a new induction machine model in the (α/β) reference frame. Its state variables are non-sinusoidal in steady state. The application a backstepping control design method results in a control structure in which a speed control is in series with a torque control in one side and a magnetic flux control is in series with a current control in the other side. A module, which adjusts the proposed control structure parameters, ensures the robustness to the system in closed loop and a good tracking performance in the presence of changes in machine resistances and inductances due to the temperature and magnetic core saturation. Simulation results show that good transient and steady state robust performances are achieved.

A novel indirect adaptive control coupled with a novel identification method for induction machine parameters is currently under investigation to ensure that the system remains stable when machine inductances change over a wide range. An observer to estimate unmeasurable state variables is also under investigation to extend the proposed control structure to squirrel cage induction motors.

References

- Accetta, A., Alonge, F., Cirrincione, M., Pucci, M. and Sferlazza, A. (2016) 'Feedback linearizing control of induction motor considering magnetic saturation effects', *IEEE Transactions on Industry Applications*, Vol. 52, No. 6, pp.4843–4854.
- Aichi, B., Bourahla, M., Kendouci, K. and Mazari, B. (2020) 'Real-time nonlinear speed control of an induction motor based on a new advanced integral backstepping approach', *Transactions of the Institute of Measurement and Control*, Vol. 42, No. 2, pp.244–258.
- Alonge, F., Cirrincione, M., Pucci, M. and Sferlazza, A. (2015) 'Input–output feedback linearization control with on-line MRAS-based inductor resistance estimation of linear induction motors including the dynamic end effects', *IEEE Transactions on Industry Applications*, Vol. 52, No. 1, pp.254–266.
- Barut, M., Demir, R., Zerdali, E. and Inan, R. (2011) 'Real-time implementation of bi input extended Kalman filter-based estimator for speed-sensorless control of induction motors', *IEEE Trans. Ind. Electron.* Vol. 59, No.11, pp.4197–4206.
- Belkheiri, M. and Boudjema, F. (2008) 'Neural network augmented backstepping control for an induction machine', *International Journal of Modelling, Identification and Control*, Vol. 5, No. 4, pp.288–296.
- Bousserhane, I.K., Hazzab, A., Rahli, M., Kamli, M. and Mazari, B.B. (2006) 'Direct field-oriented control using backstepping strategy with fuzzy rotor resistance estimator for induction motor speed control', *Information Technology and Control*, Vol. 35, No. 4.

- Chen, J. and Huang, J. (2016) 'Online decoupled stator and rotor resistances adaptation for speed sensorless induction motor drives by a time-division approach', *IEEE Transactions on Power Electronics*, Vol. 32, No. 6, pp.4587–4599.
- Chiasson, J. (1993) 'Dynamic feedback linearization of the induction motor', *IEEE Transactions on Automatic Control*, Vol. 38, No. 10, pp.1588–1594.
- Chiasson, J. (1998) 'A new approach to dynamic feedback linearization control of an induction motor', *IEEE Transactions on Automatic Control*, Vol. 43, No. 3, pp.391–397.
- Costa, B.L.G., Graciola, C.L., Angélico, B.A., Goedtel, A. and Castoldi, M.F. (2018) 'Metaheuristics optimization applied to PI controllers tuning of a DTC-SVM drive for three-phase induction motors', *Applied Soft Computing*, Vol. 62, pp.776–788.
- Depenbrock, M. (1987) 'Direct self-control (DSC) of inverter fed induction machine', *1987 IEEE Power Electronics Specialists Conference*, pp.632–641, IEEE.
- Derouich, A. and Lagrioui, A. (2014) 'Real-time simulation and analysis of the induction machine performances operating at flux constant', *International Journal Advanced Computer Science and Applications*, Vol. 5, No. 4, pp.59–64.
- Dos Santos, T.H., Goedtel, A., Da Silva, S.A.O. and Suetake, M. (2014) 'Scalar control of an induction motor using a neural sensorless technique', *Electric Power Systems Research*, Vol.108, pp.322–330.
- Ebrahim, A. and Murphy, G. (2010) 'Adaptive backstepping control of a speed-sensorless induction motor under time-varying load torque and rotor resistance uncertainty', *International Journal of Adaptive and Innovative Systems*, Vol. 1, No. 2, pp.171–186.
- El Ouanjli, N., Derouich, A., El Ghzizal, A., Chebabhi, A. and Taoussi, M. (2017) 'A comparative study between FOC and DTC controls of the doubly fed induction motor (DFIM)', *International Conference on Electrical and Information Technologies (ICEIT)*, IEEE, pp.1–6.
- Fateh, M. and Abdellatif, R. (2017) 'Comparative study of integral and classical backstabbing controllers in IFOC of induction motor fed by voltage source inverter', *International Journal of Hydrogen Energy*, Vol. 42, No. 28, pp.17953–17964.
- Fattah, H.A., Abdel, Loparo, K.A. and Emara, H.M. (1999) 'Induction motor control system performance under magnetic saturation', *Proceedings of the 1999 American Control Conference (Cat. No. 99CH36251)*, IEEE, Vol. 3, pp.1668–1672.
- Hajji, S., Ayadi, A., Agerbi Zorgani, Y., Maatoug, T., Farza, M. and M'saad, M. (2019) 'Integral backstabbing-based output feedback controller for the induction motor', *Transactions of the Institute of Measurement and Control*, Vol. 41, No. 16, pp.4599–4612.
- Hinkkanen, M., Repo, A. K and Luomi, J. (2006) 'Influence of magnetic saturation on induction motor model selection', *XVII International Conference on Electrical Machines (ICEM2006)*.
- Horch, M., Boumediene, A. and Baghli, L. (2017) 'MRAS-based sensorless speed integral backstepping control for induction machine, using a flux backstepping observer', *International Journal of Power Electronics and Drive Systems*, Vol. 8, pp.1650–1662.
- Horch, M., Boumediène, A. and Baghli, L. (2019) 'Sensorless high-order sliding modes vector control for induction motor drive with a new adaptive speed observer using super-twisting strategy', *International Journal of Computer Applications in Technology*, Vol. 60, No. 2, pp.144–153.
- Huynh, D.C. and Dunnigan, M.W. (2012) 'Advanced particle swarm optimisation algorithms for parameter estimation of a single-phase induction machine', *International Journal of Modelling, Identification and Control*, Vol. 15, No. 4, pp.227–240.
- Jannati, M., Anbaran, S.A., Asgari, S.H., Goh, W.Y., Monadi, A., Aziz, M.J.A. and Idris, N.R.N. (2017) 'A review on variable speed control techniques for efficient control of single-phase induction motors: evolution, classification, comparison', *Renewable and Sustainable Energy Reviews*, Vol. 75, pp.1306–1319.
- Khalil, H.K. and Grizzle, J.W. (2002) *Nonlinear Systems*, Prentice Hall, Upper Saddle River, NJ.
- Krstic, M., Kokotovic, P.V. and Kanellakopoulos, I. (1995) *Nonlinear and Adaptive Control Design*, John Wiley and Sons, Inc.
- Li, Q., Lin, Y., Lin, R.C. and Meng, H.F. (2019) 'Using self-constructing recurrent fuzzy neural networks for identification of nonlinear dynamic systems', *International Journal of Modelling, Identification and Control*, Vol. 33, No. 4, pp.378–386.
- Liu, L., Qiang, J.P. and Fang, Y.M. (2020) 'Modelling and dynamic surface backstepping recursive sliding mode control for the speed and tension system of the reversible cold strip rolling mill', *International Journal of Modelling, Identification and Control*, Vol. 35, No. 2, pp.93–107.
- Mapelli, F., Tarsitano, D. and F. Cheli, (2017) 'MRAS rotor resistance estimators for EV vector-controlled induction motor traction drive: analysis and experimental results', *Electric Power Systems Research*, Vol. 146 pp.298–307.
- Marino, R., Tomei, P. and Verrelli, C.M. (2010) *Induction Motor Control Design*, Springer Science and Business Media.
- Mehazzem, F., Nemmour, A.L., Reama, A. and Benalla, H. (2011) 'Nonlinear integral backstabbing control for induction motors', *International Aegean Conference on Electrical Machines and Power Electronics and Electromotion, Joint Conference*, IEEE, pp.331–336.
- Mengoni, M., Agarlita, S.C., Zarri, L. and Casadei, D. (2012) 'On-line estimation of stator resistance and mutual inductance of multiphase induction machines', *2012 13th International Conference on Optimization of Electrical and Electronic Equipment (OPTIM)*, IEEE, pp.417–423.
- Nishad, B.K. and Sharma, R. (2018) 'Induction motor control using modified indirect field-oriented control', *2018 8th IEEE India International Conference on Power Electronics (IICPE)*, IEEE, pp.1–5.
- Okou, F.A., Nganga-Kouya, D. and Tarbouchi, M. (2009) 'A backstabbing approach for the design of a nonlinear controller for a two-wheeled autonomous vehicle', *2009 Canadian Conference on Electrical and Computer Engineering*, IEEE, pp.641–645.
- Ouadi, H., Giri, F. and Ikhouane, F. (2002) 'Backstepping control of saturated induction motors', *15th Triennial World Congress, IFAC*.
- Regaya, C.B., Farhani, F., Zaafouri, A. and Chaari, A. (2012) 'Comparison between twomethod for adjusting the rotor resistance', *International Review on Modelling and Simulations*, Vol. 5, No. 2.

- Saad, K., Abdellah, K., Ahmed, H. and Iqbal, A. (2019) 'Investigation on SVM-backstepping sensorless control of five-phase open-end winding induction motor based on model reference adaptive system and parameter estimation', *Engineering Science and Technology, an International Journal*, Vol. 22, No. 4, pp.1013–1026.
- Saravanan, M.C., Azarudeen, A.M., and Selvakumar, S (2012) 'Performance of three phase induction motor using modified stator winding', *Global Journal of Research in Engineering*, Vol. 12, No. 5-F.
- Takahashi, I. and Noguchi, T. (1986) 'A new quick-response and high efficiency control strategy of an induction motor', *IEEE Transactions on Industry Applications*, No. 5, pp.820–827.
- Traoré, D., Leon, D. and Glumineau, A. (2012) 'Adaptive interconnect observer-based backstepping control design for sensorless induction motor', *Automatica*, Vol. 48, No. 4, pp.682–687.
- Xu, D., Huang, J., Su, X. and Shi, P. (2019) 'Adaptive command-filtered fuzzy backstepping control for linear induction motor with unknown end effect', *Information Sciences*, Vol. 477, pp.118–131.
- Yang, S., Ding, D., Li, X., Xie, Z., Zhang, X. and Chang, L. (2018) 'A decoupling estimation scheme for rotor resistance and mutual inductance in indirect vector-controlled induction motor drives', *IEEE Transactions on Energy Conversion*, Vol. 34, No. 2, pp.1033–1042.
- Zhao, L., Huang, J., Liu, H., Li, B. and Kong, W. (2014) 'Second-order sliding-mode observer with online parameter identification for sensorless induction motor drives', *IEEE Transactions on Industrial Electronics*, Vol. 61, No. 10, pp.5280–5289.